CONSTRAINTS ON THE DEPTH OF ORIGIN OF BASIN RINGS AND THE COMPOSITION OF THE LUNAR CRUST USING THE KAGUYA MULTIBAND IMAGER. M. Lemelin[1], P.G. Lucey[1], L.R. Gaddis[2], K. Miljković[3], and M. Ohtake[4], [1]Hawaii Institute of Geophysics and Planetology, Department of Geology and Geophysics, University of Hawaii at Manoa, 1680 East-West Rd, POST 602, Honolulu, HI 96822, USA, mlemelin@hawaii.edu, [2]Astrogeology Science Center, United States Geological Survey, Flagstaff, AZ 86001, USA, [3]Department of Applied Geology, Curtin University, GPO Box U1987, Perth WA 6845, Australia, [4]Institute of Space and Astronautical Science, Japan Aerospace Exploration Agency, Sagamihara, Kanagawa 252-5210, Japan.

Introduction: The mineralogical composition of the lunar crust across the entire surface and at a wide range of depths can be inferred from remote sensing observations of complex craters and impact basins on the Moon. Complex impact craters expose material in their central peak, which originates from a depth of ~0.1*D* within the crust [1] (where *D* is the transient crater diameter). However, the depth of origin of the material exposed in the ring(s) of impact basins is not well understood, with some estimates ranging from about ~0.035*D* [2] to ~0.15*D* [3]. Placing better constraints on the depth of origin of material exposed by the basin's innermost ring (which likely represents the deepest derived material in multi-ring basins [1]) would be of great value because it would allow to use the mineralogical analysis of basin rings in concert with that of central peaks in an attempt to assess the composition of the lunar crust.

Recent studies suggest there is a striking difference in composition between the rock population of central peaks [e.g., 4-9] and basin rings [e.g., 7,10,11]. For example, Lemelin et al. [9] found that central peaks in the Feldspathic Highland Terrane (FHT), which expose material throughout the entire crustal column, from 5 to 49 km above the crust/mantle boundary, are on average composed of anorthosites, noritic or gabbroic anorthosites, and anorthositic norites or gabbros. They report small local exposures of purest anorthosite (plagioclase content ≥98 wt.%). On the other hand, global surveys identified local exposures of norites, troctolites, and purest anorthosites [e.g., 3,7,10,11] in and around many impact basins.

Our objective is to better constrain the composition of the lunar crust with depth by (1) conducting a comprehensive study of the mineralogy of the basin's innermost ring such as that of Cheek et al. [12] for 13 basins, and comparing their mineralogy to that of the central peaks studied by Lemelin et al. [9], and by (2) using iSALE-2D hydrocode models to better constrain the depth of origin of the material exposed by the basin's innermost ring. The basins we study are: Crisium, Freundlich-Sharon, Hertzsprung, Humorum, Imbrium, Korolev, Lorentz, Mendeleev, Mendel-Rydberg, Moscoviense, Nectaris, Orientale, and Serenitatis.

Methods and datasets: We identified the innermost ring for each of the basins using the Bouguer gravity anomaly from the Gravity Recovery And Interior Laboratory (GRAIL), and lunar geologic maps from the United States Geological Survey (USGS) [13]. We defined the innermost ring material as the USGS "circumbasin materials" or "basin materials" located within a basin's Bouguer gravity anomaly.

We determined the composition of the innermost ring of these basins at ~80 m/pixel for all immature exposures (OMAT>0.2 [14]), using Multiband Imager data (750-1550nm, MAP level 02 [15]) and Hapke's radiative transfer equations. We constructed a spectral lookup table of the reflectance spectra of 6601 mixtures of olivine, orthopyroxene, clinopyroxene and plagioclase, at 7 amounts of submicroscopic iron (SMFe), an Mg# (Mg/Mg+Fe) of 65, and a grain size of 17µm. We also modeled the reflectance spectra of these mixtures for a grain size of 200 µm for plagioclase to account for the band depth observed in the Multiband Imager data [5], for a total of 92,414 spectra. We compared the modeled spectra that contained ±2 wt% FeO of a given pixel [9], and assigned the composition to the best spectral match (in terms of correlation and absolute difference in continuum removed reflectance).

We modeled the depth of origin (D_o) of the material exposed by the innermost rings using iSALE-2D. The spatial sampling of these models does not allow direct detection of the rings, but rather a zone that would include the rings (the top 10 km of the region of crustal thinning). We find this region exposes material originating principally from two depths: a "shallow component" from the crust, a "deep component" from the lower crust or the upper mantle. There is also a component from the impactor. The relative abundances of these components depend on the impactor size, speed and pre-impact crustal thickness. In this initial model, we assume a cold impact target [16].

Initial results: Impact modeling suggests that the shallow and the deep component have a depth of origin of ~0.07*D* and ~0.22*D* respectively (Fig. 1). While the models do show the proportions of components found in the region where rings would form (the top 10 km of the region of crustal thinning), we do not assume that the rings themselves reflect these proportions (hence average composition). In figure 2a, we plot the prox-

imity to the mantle of the shallow and deep components, and the average plagioclase content of the rings. The rings appear to be largely dominated by the shallow component, as a major contribution by the deep component would imply a plagioclase-rich mantle.

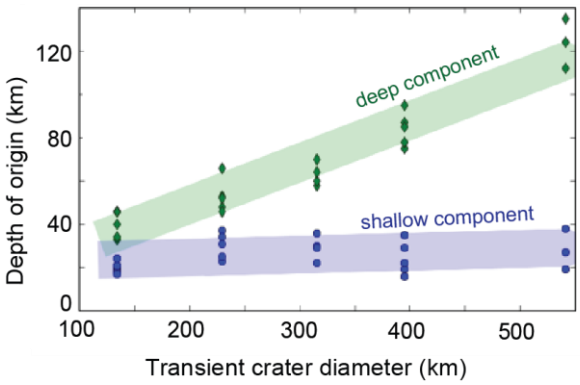

Figure 1. Modeling the mean depth of origin of the material exposed by the innermost ring, using the top 10 km of crustal thinning region as a proxy for the location of the innermost ring (assuming pre-impact crustal thicknesses of 30, 45, 60 km, and cold target [16]).

We find that of the 13 basins, 3 excavated only crustal material (both the shallow and deep components are from the crust): Hertzsprung, Korolev and Mendeleev. The innermost ring of these basins exposes material from similar depths, 3 to 34 km above the crust/mantle boundary (pre-impact crustal thickness – depth of origin). These rings also have very similar average abundances of plagioclase (92-93 wt.%), clinopyroxene (3-4 wt.%), orthopyroxene (2-3 wt.%), and olivine (2 wt.%), suggesting that the crust is quite homogeneous and anorthositic where these basins are located on the lunar far side.

According to our model, the deep component of the 10 other basins comes from the upper mantle (*i.e.*, 0.22*D*>pre-impact crustal thickness) (Fig. 2a). However, these basins contain too much plagioclase (≥67 wt.%) for that to be reasonable. Instead, if we assume that 100% of the ring material comes from the shallow component (Fig. 2a), we can reconcile the mineralogy of the basin rings in this study and that of the central peaks studied by Lemelin et al. [9] (Fig. 2b).

We also find that 2 to 34% of the pixels of each basin ring have their reflectance minimum at 1.250 µm (a proxy for purest anorthosite), Orientale is an exception with 46%; purest anorthosite is detected in all basins.

Acknowledgments: This work was supported by the NASA Lunar Advanced Science and Exploration Research (LASER) grant NNX12AI78G (P.G. Lucey, PI), and by the Natural Science and Engineering Council of Cananda (NSERC).

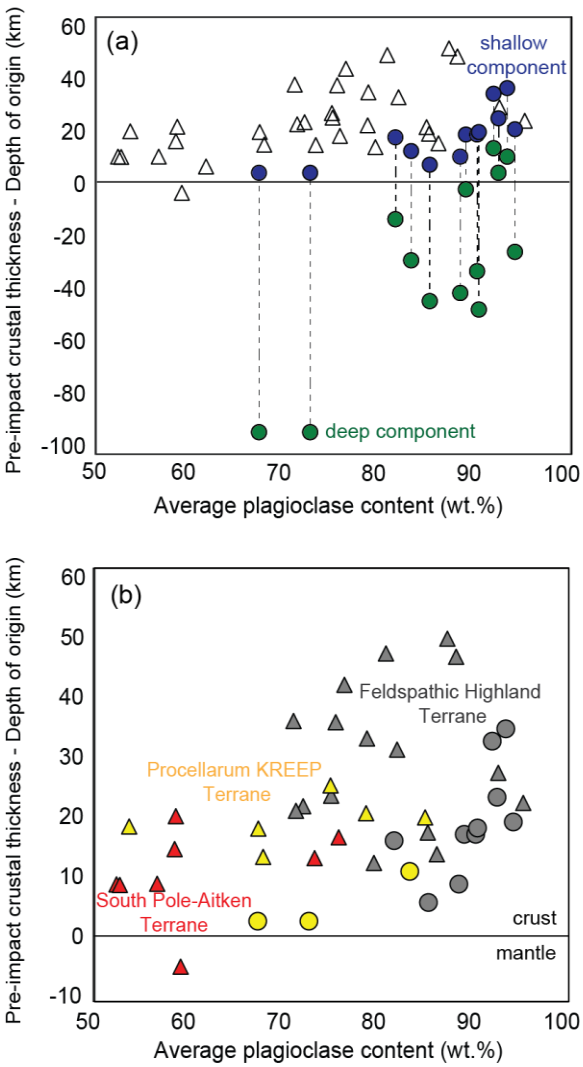

Figure 2. Average plagioclase content of the basin's innermost ring in this study (circles) and the central peaks studied by Lemelin et al. (2015) (triangles), versus their proximity to the crust mantle boundary (horizontal line). (a) The average plagioclase content of each basin (circles) is shown at the location of the shallow (blue) and deep (green) component. (b) The average plagioclase content of each basin (circles) is assigned to the depth of origin of the shallow component. The color represent the geological terrane.

References: [1] Melosh, H.J. (1989) Impact Cratering: A Geologic Process, Oxford monographs on Geology and Geophysics no. 11, Oxford Univ. Press, New York. [2] Crites, S.T. et al. (2015) *American Mineralogist, 100*, 1708-1716. [3] Baker, D.M.H. and Head, J.W. (2015) Icarus, 258, 164-180. [4] Tompkins, S. and Pieters, C.M. (1999) Meteorit. Planet. Sci., 34, 25-41. [5] Ohtake, M. et al. (2009) Nature, 461, 236-241. [6] Cahill, J.S.T. et al., (2009) JGR, 114, E09001. [7] Donaldson Hanna, K.L. et al. (2014) JGR, 119, 1516-1545. [8] Song, E. et al. (2013) JGR, 118, 689-707. [9] Lemelin, M. et al. (2015) JGR, 120, 869-887. [10] Yamamoto, S. et al. (2010) NGL, 3, 533-536. [11] Yamamoto, S. et al. (2012) GRL, 39, L13201. [12] Cheek, L.C. et al. (2013) JGR, 118, 1805-1820. [13] Fortezzo and Hare (2013) 44th LPSC, abstract 2144. [14] Lucey, P.G. et al. (2000) JGR, 105, 20377-20386. [15] Ohtake, M. et al. (2008) Earth Planets Space, 60, 257-264. [16] Miljković, K. et al. (2015) EPSL, 409, 243-251.